Accurate Homogeneous Electron Gas Exchange-Correlation Free Energy for Local Spin-Density Calculations

Valentin V. Karasiev,[1,*] Travis Sjostrom,[2] James Dufty,[3] and S. B. Trickey[1]
[1]Quantum Theory Project, Departments of Physics and of Chemistry, University of Florida, Gainesville, Florida 32611-8435, USA
[2]Theoretical Division, Los Alamos National Laboratory, Los Alamos, New Mexico 87545, USA
[3]Department of Physics, University of Florida, Gainesville, Florida 32611-8435, USA
(Received 19 November 2013; published 20 February 2014)

An accurate analytical parametrization for the exchange-correlation free energy of the homogeneous electron gas, including interpolation for partial spin polarization, is derived via thermodynamic analysis of recent restricted path integral Monte Carlo (RPIMC) data. This parametrization constitutes the local spin density approximation (LSDA) for the exchange-correlation functional in density functional theory. The new finite-temperature LSDA reproduces the RPIMC data well, satisfies the correct high-density and low- and high-T asymptotic limits, and is well behaved beyond the range of the RPIMC data, suggestive of broad utility.

DOI: 10.1103/PhysRevLett.112.076403 PACS numbers: 71.15.Mb, 05.70.Ce, 31.15.E-, 65.40.G-

The homogeneous electron gas (HEG) is a fundamentally important system for understanding many-fermion physics. In the absence of exact analytical solutions for its energetics, high-precision numerical results have been critical to insight. Recently published [1] restricted path integral Monte Carlo (RPIMC) data for the HEG over a wide range of temperatures and densities open the opportunity to obtain closed form expressions for HEG thermodynamics, in particular, the exchange and correlation (XC) contributions. Such expressions extracted from Monte Carlo data are well known for the zero-T HEG, where they have played a major role in understanding inhomogeneous electron-system behavior. We provide the corresponding thermodynamical expressions for wide temperature and density ranges.

Density functional theory (DFT) is the motivating context. For ground-state DFT, the most basic XC density functional is the local density approximation (LDA). It approximates the local XC energy per particle, $\varepsilon_{\rm xc}$, as the value for the HEG at the local density, $\varepsilon_{\rm xc}^{\rm LDA}(n(\mathbf{r})) \approx \varepsilon_{\rm xc}^{\rm HEG}(n)|_{n=n(\mathbf{r})}$ [see, also, Eq. (3) below]. Computational implementation is via parametrizations [2,3] of HEG quantum Monte Carlo (QMC) data [4]. Recent QMC results [5] for the spin-polarized $T = 0$ K HEG also validate the spin-interpolation formulas used in that case, the local spin density approximation (LSDA). All more-refined $\varepsilon_{\rm xc}$ approximations reduce to the LSDA in the weak inhomogeneity limit.

Finite-temperature DFT [6–8] increasingly is being used to study matter under diverse density and temperature conditions [9–14]. In it, the XC free energy is defined by decomposition of the universal free-energy density functional (independent of the external potential). With the T-dependence suppressed for now, that functional is

$$\mathcal{F}[n] = \mathcal{T}_{\rm s}[n] - T\mathcal{S}_{\rm s}[n] + \mathcal{F}_{\rm H}[n] + \mathcal{F}_{\rm xc}[n]. \quad (1)$$

The first two terms are the noninteracting kinetic energy and entropy (also known as the Kohn-Sham KE and entropy), $\mathcal{F}_{\rm H}[n]$ is the classical electron-electron Coulomb energy, and the XC free energy by definition is

$$\mathcal{F}_{\rm xc}[n] \coloneqq (\mathcal{T}[n] - \mathcal{T}_{\rm s}[n]) - T(\mathcal{S}[n] - \mathcal{S}_{\rm s}[n]) + (\mathcal{U}_{\rm ee}[n] - \mathcal{F}_{\rm H}[n]), \quad (2)$$

with $\mathcal{T}[n]$ and $\mathcal{S}[n]$ the interacting system kinetic energy and entropy and $\mathcal{U}_{\rm ee}[n]$ the full quantum mechanical electron-electron interaction energy.

Just as for $T = 0$ K, the existence theorems of finite-T DFT are not constructive for $\mathcal{F}_{\rm xc}$, so approximations must be devised. Common practice [9] in simulations is to use a $T = 0$ K XC functional, $\mathcal{F}_{\rm xc}[n(T), T] \approx E_{\rm xc}[n(T)]$. This gives only the implicit T dependence provided by $n(\mathbf{r}, T)$. However, there is substantial evidence from both finite-T Hartree-Fock [12,15] and finite-T exact exchange calculations [16,17] of non-negligible T dependence in exchange itself.

Addressing that T dependence until now has been hampered by lack of an accurate, simulation-based LDA for $\mathcal{F}_{\rm xc}$. Thus, several $\mathcal{F}_{\rm xc}$ approximations have been proposed on the basis of various models; see Ref. [18] and references therein. The RPIMC data for the HEG in Ref. [1] provide the opportunity to fill that gap with a LSDA on equivalent footing with the ground-state $E_{\rm xc}^{\rm LSDA}$. Note that Ref. [19] provided a fit for the RPIMC XC internal energy data but not for $\mathcal{F}_{\rm xc}$. Subsequently, an error in that fit was corrected. Here we use the corrected fit denoted as "BDHC." Incidental to the main theme of Ref. [18], two of us fitted the unpolarized finite-T

RPIMC results [1] and extracted a parametrization of the HEG XC free energy. That constitutes a LDA $\mathcal{F}_{\rm xc}$. But several important issues were not treated; namely, which of the several possible thermodynamic routes is optimal for extracting $\mathcal{F}_{\rm xc}$, what functional form is the most reliable for the requisite fitting of the RPIMC data, which RPIMC data to use, and how to handle the partially polarized case. We address those here to provide the free-energy LDA and LSDA with full T dependence,

$$\begin{aligned}\mathcal{F}_{\rm xc}[n(T),T] &= \int d\mathbf{r} n(\mathbf{r},T) f_{\rm xc}[n(T);\mathbf{r},T] \\ &\approx \int d\mathbf{r} n(\mathbf{r},T) f_{\rm xc}^{\rm HEG}(n(\mathbf{r},T),T) \\ &\equiv \mathcal{F}_{\rm xc}^{\rm LSDA}[n(T),T], \end{aligned} \tag{3}$$

where $f_{\rm xc}^{\rm HEG}(n,T) = F_{\rm xc}^{\rm HEG}(n,T)/N$ is the XC free energy per particle for the HEG and N the electron number. Note that at $T = 0$ K, $f_{\rm xc} = \varepsilon_{\rm xc}$ and $\mathcal{F}_{\rm xc} = E_{\rm xc}$.

Unless noted otherwise, we use Hartree atomic units. (Observe that Refs. [1,19] use Rydberg a.u.) The interacting HEG is described completely by three parameters: the density $n^{\rm HEG} = n = N/V$, spin polarization $\zeta = (n_\uparrow - n_\downarrow)/n$, and temperature T. Its XC free energy per particle $f_{\rm xc}^{\rm HEG}(n^{\rm HEG},T) = \mathcal{F}_{\rm xc}^{\rm HEG}[n^{\rm HEG},T]/N$ is the quantity of interest. As usual, we use the Wigner-Seitz radius, $r_{\rm s} = (3/4\pi n)^{1/3}$, and reduced temperature $t = T/T_F$, with the Fermi temperature $T_F^{\zeta=0} = [3\pi^2 n]^{2/3}/2k_B$ for the unpolarized case and $T_F^{\zeta=1} = [6\pi^2 n]^{2/3}/2k_B$ for the fully polarized case. Significant densities range from $r_{\rm s} \ll 1$ through $r_{\rm s} \geq 10$. The relevant temperature range is at least $0 \leq t \leq 10$. While large t represents the classical limit, the approach to it will vary with $r_{\rm s}$, via the dimensionless Coulomb coupling parameter, $\Gamma = 2\lambda^2 r_{\rm s}/t$ with $\lambda = (4/9\pi)^{1/3}$.

The RPIMC data for the HEG [1] are the total kinetic $\mathcal{T}$ and potential (or interaction) $\mathcal{U}_{\rm ee}$ energies for given $r_{\rm s}$ and t. The issues are which RPIMC data to use and how best to extract a broadly reliable $f_{\rm xc}$ from those data.

One thermodynamic route is via the RPIMC data for the XC internal energy per particle, which is the difference of the interacting and noninteracting system total internal energies per particle, $\varepsilon_{\rm xc} = \tau + u_{\rm ee} - \tau_{\rm s}$, with $\tau = \mathcal{T}/N$, $u_{\rm ee} = \mathcal{U}_{\rm ee}/N$, and $\tau_{\rm s} = \mathcal{T}_{\rm s}/N$ the noninteracting HEG kinetic energy per particle (i.e., $\mathcal{T}_{\rm s}$ is the finite-T Thomas-Fermi KE [20,21]). Observe that $\tau_{\rm s}$ is given both analytically and tabularly in the Supplemental Material for Ref. [1]. From Eq. (2) $f_{\rm xc} = \varepsilon_{\rm xc} - T\sigma_{\rm xc}$, which with a standard thermodynamic relation for the entropic contribution per particle

$$\sigma_{\rm xc}(r_{\rm s},t) = -\frac{t}{T}\frac{\partial f_{\rm xc}(r_{\rm s},t)}{\partial t}\bigg|_{r_{\rm s}} \tag{4}$$

gives

$$f_{\rm xc}(r_{\rm s},t) - t\frac{\partial f_{\rm xc}(r_{\rm s},t)}{\partial t}\bigg|_{r_{\rm s}} = \varepsilon_{\rm xc}(r_{\rm s},t). \tag{5}$$

Observe that the $\mathcal{F}_{\rm H}$ from Eq. (2) vanishes for the HEG because of the neutralizing background.

Reference [18] used another thermodynamic relation to obtain $f_{\rm xc}$ directly from the RPIMC interaction energy $u_{\rm ee}$ per particle via integration over Γ, the coupling constant [22]. This is equivalent [23] to

$$f_{\rm xc}(r_{\rm s},t) = \frac{1}{r_{\rm s}^2}\int_0^{r_{\rm s}} dr_{\rm s}' r_{\rm s}' u_{\rm ee}(r_{\rm s}',t)|_t. \tag{6}$$

Exact integration requires the choice of an integrable form fitted to the RPIMC data for $u_{\rm ee}$. Instead, differentiation of Eq. (6) with respect to $r_{\rm s}$ gives

$$2f_{\rm xc}(r_{\rm s},t) + r_{\rm s}\frac{\partial f_{\rm xc}(r_{\rm s},t)}{\partial r_{\rm s}}\bigg|_t = u_{\rm ee}(r_{\rm s},t), \tag{7}$$

which is the analogue of Eq. (5). Equations (5) and (7) may be combined to yield

$$\begin{aligned}\tau_{\rm s}(r_{\rm s},t) - t\frac{\partial f_{\rm xc}(r_{\rm s},t)}{\partial t}\bigg|_{r_{\rm s}} \\ - f_{\rm xc}(r_{\rm s},t) - r_{\rm s}\frac{\partial f_{\rm xc}(r_{\rm s},t)}{\partial r_{\rm s}}\bigg|_t = \tau(r_{\rm s},t).\end{aligned} \tag{8}$$

Fitting a suitable analytical $f_{\rm xc}(r_{\rm s},t)$ to one of Eqs. (5), (7), or (8) constitutes our fits A, B, and D, respectively. While fits B and D each use only one subset of the RPIMC data ($u_{\rm ee}$, τ, respectively), fit A uses both via the combination $\varepsilon_{\rm xc}$. A second way to use both data sets is to fit $f_{\rm xc}$ to Eqs. (7) and (8) concurrently; this is our fit C. All four fits use the RPIMC data on its discrete mesh, while the assumed functional form for $f_{\rm xc}$ should provide useful extrapolation outside the RPIMC data domain. Brown *et al.* used [19] a functional form similar to the Perrot–Dharma-wardana [24] XC functional to fit the RPIMC data for $\varepsilon_{\rm xc}$. We tested both the original and Brown *et al.* versions and found physically implausible behavior (oscillations) in the $r_{\rm s}$ dependence. See the Supplemental Material [25].

A Padé approximant as originally given by Ichimaru and co-workers [22,26–28] and also employed in Ref. [18] for $u_{\rm ee}$ is suggestive. We used an extension of that form for $f_{\rm xc}$ (rather than $u_{\rm ee}$) for both the unpolarized and fully polarized cases. With explicit polarization labeling, the form is

$$f_{\rm xc}^{\zeta}(r_{\rm s},t) = -\frac{1}{r_{\rm s}}\frac{\omega_\zeta a(t) + b_\zeta(t) r_{\rm s}^{1/2} + c_\zeta(t) r_{\rm s}}{1 + d_\zeta(t) r_{\rm s}^{1/2} + e_\zeta(t) r_{\rm s}}, \tag{9}$$

where $\omega_0 = 1$ and $\omega_1 = 2^{1/3}$ for $\zeta = 0$, 1, respectively. The functions $a(t)$, $b_\zeta(t) - e_\zeta(t)$, in turn, are Padé

approximants in t. The original forms [28] proved to be inadequate to reproduce the RPIMC ε_{xc} data at $r_s = 1$. This inflexibility was remedied by adding one parameter in $c_\zeta(t)$, with the resulting definitions for $a(t)$, $b_\zeta(t)$–$e_\zeta(t)$ as follows (ζ labeling suppressed for clarity):

$$a(t) = 0.610\,887 \tanh\left(\frac{1}{t}\right) \times \frac{0.75 + 3.043\,63t^2 - 0.092\,27t^3 + 1.7035t^4}{1 + 8.310\,51t^2 + 5.1105t^4}, \tag{10}$$

$$b(t) = \tanh\left(\frac{1}{\sqrt{t}}\right) \frac{b_1 + b_2 t^2 + b_3 t^4}{1 + b_4 t^2 + b_5 t^4}, \tag{11}$$

$$c(t) = \left[c_1 + c_2 \exp\left(-\frac{c_3}{t}\right)\right] e(t), \tag{12}$$

$$d(t) = \tanh\left(\frac{1}{\sqrt{t}}\right) \frac{d_1 + d_2 t^2 + d_3 t^4}{1 + d_4 t^2 + d_5 t^4}, \tag{13}$$

$$e(t) = \tanh\left(\frac{1}{t}\right) \frac{e_1 + e_2 t^2 + e_3 t^4}{1 + e_4 t^2 + e_5 t^4}. \tag{14}$$

In the small-r_s and small-Γ limits, Eq. (9) reduces to the finite-T X functional of Ref. [29] (see, also, Refs. [22,26] for details),

$$f_x^\zeta(r_s, t) = -\frac{\omega_\zeta}{r_s} a(t). \tag{15}$$

The correct $T = 0$ K limit is obtained by using the recent $T = 0$ K QMC data [5]. Thus, Eq. (9) first was fitted at $t = 0$ to the zero-T QMC data, which fixed the parameters b_1, c_1, d_1, and e_1. The remaining parameters in Eq. (9) were fitted to the finite-T RPIMC data. The correct high-T limit,

$$\lim_{T\to\infty} f_{xc}^\zeta(r_s, t) = -\frac{1}{\sqrt{3}} r_s^{-3/2} T^{-1/2} + O(T^{-1}), \tag{16}$$

for all ζ corresponds to the leading correlation term; see Refs. [29–31]. It was incorporated by fixing the ratio between the parameters $b_{\zeta,5} = \sqrt{3/2}\omega_\zeta \lambda^{-1} b_{\zeta,3}$ in $b_\zeta(t)$.

Each of the thermodynamic routes A, B, C, or D to f_{xc} from a RPIMC data subset can be tested by computing values for both the subset used in that fit and the unused subsets and comparing the results with the original RPIMC data. For example, fit A uses RPIMC ε_{xc} data as input to Eq. (5). Thus, we calculated values of u_{ee}^{fit} via Eq. (7) and τ^{fit} via Eq. (8) from the fit A f_{xc} and compared the results to the RPIMC data in the form of mean absolute relative errors (MARE). The essential result is that fits A and C are close in quality, but fit A is modestly better on the grounds of MARE for ε_{xc}. From the same perspective, the resulting fit to ε_{xc} also is better than the BDHC fit. The final parameters are shown in Table I and error comparisons are in Table II. [Those parameters were done with analytical derivatives in Eq. (5), after exploration of fits with numerical thermodynamic derivatives.] Other error comparisons are in the Supplemental Material [25].

TABLE I. Fit A parameters for the XC free-energy functional for the unpolarized ($\zeta = 0$) and fully polarized ($\zeta = 1$) HEG.

	$\zeta = 0$	$\zeta = 1$
b_1	0.283 997	0.329 001
b_2	48.932 154	111.598 308
b_3	0.370 919	0.537 053
b_4	61.095 357	105.086 663
b_5	$\sqrt{3/2}\lambda^{-1}b_3 = 0.871\,837$	$\sqrt{3/2}2^{1/3}\lambda^{-1}b_3 = 1.590\,438$
c_1	0.870 089	0.848 930
c_2	0.193 077	0.167 952
c_3	2.414 644	0.088 820
d_1	0.579 824	0.551 330
d_2	94.537 454	180.213 159
d_3	97.839 603	134.486 231
d_4	59.939 999	103.861 695
d_5	24.388 037	17.750 710
e_1	0.212 036	0.153 124
e_2	16.731 249	19.543 945
e_3	28.485 792	43.400 337
e_4	34.028 876	120.255 145
e_5	17.235 515	15.662 836

Figure 1 shows XC free f_{xc} and internal ε_{xc} energies per particle from fit A for $r_s = 1$, 2, and 40 over $0.01 \le t \le 1000$, with the ε_{xc} energies per particle compared to the RPIMC data. The ε_{xc} calculated with the

TABLE II. RPIMC data sets used for fits with MARE and absolute maximum relative errors (%) for calculated kinetic, interaction, and XC internal energies per particle for unpolarized ($\zeta = 0$) and fully polarized ($\zeta = 1$) cases.

Function	Fitted to	τ	u_{ee}	ε_{xc}
$\zeta = 0$				
BDHC	ε_{xc}	⋯	⋯	1.3/14
Fit A	ε_{xc}	1.3/10	1.4/4.5	0.5/3.3
Fit B	u_{ee}	1.8/6.1	0.3/1.2	1.9/9.2
Fit C	τ and u_{ee}	1.0/8.3	0.5/2.8	1.2/7.5
Fit D	τ	0.6/5.1	5.0/18	5.6/23
$\zeta = 1$				
BDHC	ε_{xc}	⋯	⋯	2.3/18
Fit A	ε_{xc}	1.7/13	1.6/4.8	1.2/7.8
Fit B	u_{ee}	2.2/15	0.5/3.7	2.2/10
Fit C	τ and u_{ee}	1.2/8.0	0.8/3.8	1.7/9.3
Fit D	τ	0.6/4.2	6.3/17	7.2/25

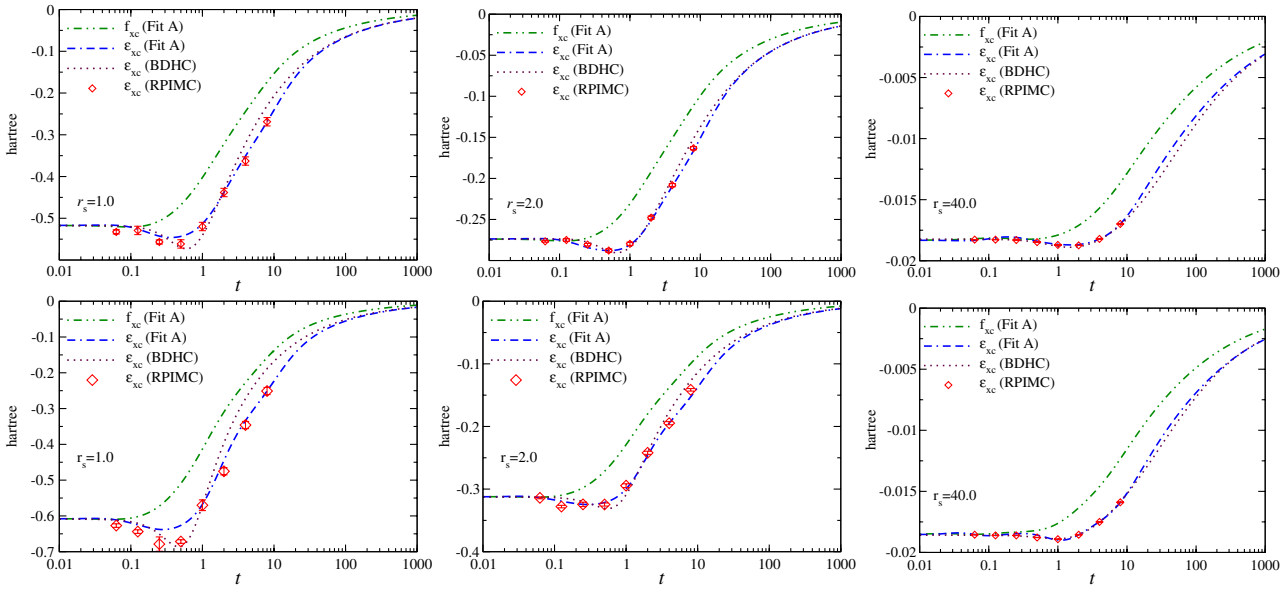

FIG. 1 (color online). $\varepsilon_{\rm xc}$ and $f_{\rm xc}$ from fit A for the unpolarized $\zeta = 0$ (top) and the fully polarized $\zeta = 1$ (bottom) HEG at $r_{\rm s} = 1$, 2, and 40 along with RPIMC data and BDHC fit for $\varepsilon_{\rm xc}$.

BDHC form [19] also is shown. The results for fit A agree as well with the RPIMC data as the BDHC fit. The $t \to 0$ limit of the entropic contribution, of course, is zero, so the fits and the RPIMC data converge to the $t = 0$ $\varepsilon_{\rm xc}$ value. The zero-T unpolarized equilibrium density $r_{\rm s} = 4.19$ from our fit is identical with the value obtained by Perdew and Wang [32]. The high-T limit is determined by Eq. (16) for all the $f_{\rm xc}$ functionals. Note that we do not attempt to have our fit describe ordered phases (e.g., Wigner crystal) at large $r_{\rm s}$. To do so would be an unwarranted extrapolation of the RPIMC data. Additional comparisons are in the Supplemental Material [25].

We now turn to intermediate polarizations. In principle, the XC functional has separate exchange and correlation contributions. At $T = 0$ K, exact spin scaling [33] defines the X functional for arbitrary polarization in terms of the unpolarized one. The argument can be extended straightforwardly to $T > 0$ K; see the Supplemental Material [25]. No corresponding exact result is known for interpolating the C contribution between $\zeta = 0$ and $\zeta = 1$, so approximate forms are used. Moreover, it is convenient computationally to use an XC functional rather than separate X and C contributions. We used such a form,

$$f_{\rm xc}(r_{\rm s}, T, \zeta) = f^0_{\rm xc}(r_{\rm s}, t) + [f^1_{\rm xc}(r_{\rm s}, 2^{-2/3}t) - f^0_{\rm xc}(r_{\rm s}, t)]\phi(r_{\rm s}, t, \zeta), \tag{17}$$

with $\phi(r_{\rm s}, t, \zeta)$ the polarization interpolation function and t on the right-hand side chosen systematically to be that of the unpolarized case, $t = T/T_F^{\zeta=0}$, as well as in Eqs. (19) and (20) below. At $T = 0$ K [34],

$$\phi(\zeta) = \frac{(1+\zeta)^\alpha + (1-\zeta)^\alpha - 2}{2^\alpha - 2}, \tag{18}$$

with $\alpha = 4/3$. Perrot and Dharma-wardana [24] developed a finite-T generalization, $\phi(r_{\rm s}, t, \zeta)$, by replacing the exponent $\alpha = 4/3$ with a function, $\alpha(r_{\rm s}, t)$, as follows:

$$\begin{aligned} \alpha(r_{\rm s}, t) &= 2 - g(r_{\rm s}) \exp\{-t\lambda(r_{\rm s}, t)\}, \\ g(r_{\rm s}) &= \frac{g_1 + g_2 r_{\rm s}}{1 + g_3 r_{\rm s}}, \\ \lambda(r_{\rm s}, t) &= \lambda_1 + \lambda_2 t r_{\rm s}^{1/2}. \end{aligned} \tag{19}$$

Their parametrization used classical map hypernetted chain (CHNC) data for the HEG and proper behavior as $T \to 0$ K. We have reparametrized $\phi(r_{\rm s}, t, \zeta)$ using the more recent $T = 0$ K QMC data (which includes intermediate polarizations $\zeta = 0.34$, 0.66) [5] along with the CHNC data for intermediate $\zeta = 0.6$ in Table IV of Ref. [24]. (Observe that this is the only use of those CHNC data in this work.) The result is a modest improvement for $T = 0$ K. The new parameter values are in Table III. The value of g_1 is fixed from the condition that $\lim_{r_{\rm s}\to 0}\phi(r_{\rm s}, t = 0, \zeta) = \phi(\zeta)$. The revised $\phi(r_{\rm s}, t, \zeta)$ depends weakly on t for all $r_{\rm s}$ and ζ.

Exact spin interpolation for finite-T exchange yields the exchange free energy

$$f_{\rm x}(r_{\rm s}, T, \zeta) = \frac{1}{2}[(1+\zeta)^{4/3} f^0_{\rm x}(r_{\rm s}, t_\uparrow) + (1-\zeta)^{4/3} f^0_{\rm x}(r_{\rm s}, t_\downarrow)], \tag{20}$$

TABLE III. Parameters for the polarization interpolation function given in Eqs. (18) and (19).

	$\nu = 1$	$\nu = 2$	$\nu = 3$
g_ν	2/3	−0.013 926 1	0.183 208
λ_ν	1.064 009	0.572 565	⋯

where $t_{\uparrow/\downarrow} \equiv t(2n_{\uparrow/\downarrow}, T) = 2k_B T/[3\pi^2(2n_{\uparrow/\downarrow})]^{2/3}$ and $n_{\uparrow/\downarrow} = (1 \pm \zeta)n/2$. [Note that f_x^ζ for $\zeta = 0$, 1 given by Eq. (15) also is given both analytically as a Fermi integral and tabulated in the Ref. [1] Supplemental Material as $E_{x,\mathrm{HF}}$.] Thus, the correlation free energy can be found from Eqs. (17) and (20) to be

$$f_c(r_s, T, \zeta) = f_{xc}(r_s, T, \zeta) - f_x(r_s, T, \zeta). \quad (21)$$

To test the $T \to 0$ K limit of our interpolation, we calculated the correlation energy per particle

$$\varepsilon_c(r_s, \zeta) \equiv f_c(r_s, 0, \zeta) = f_{xc}(r_s, 0, \zeta) - f_x(r_s, 0, \zeta), \quad (22)$$

where $f_x(r_s, 0, \zeta) \equiv \varepsilon_x(r_s, \zeta)$ is the LSDA X energy per particle. A comparison with the Perdew-Zunger (PZ) LSDA [2] and QMC simulation data shows excellent agreement as a function of ζ for $r_s = 0.25$, 0.5, 1, 2, 3, 5, 10, and 20, with the maximum relative difference between Eq. (22) and the PZ correlation energy about 4% at $r_s = 0.25$ and 0.5. (See, also, the Supplemental Material [25].)

In sum, we have extracted the XC free energy for the finite-T HEG from the RPIMC data, parametrized it in a form with exact asymptotic limits ($r_s \ll 1$, $t = 0$, and $t \gg 1$) for both the spin unpolarized and fully polarized cases, and provided a T-dependent interpolation for intermediate polarizations. The result, Eqs. (9–14) and (17–19) and associated parameters, is a proper finite-T extension of the widely used ground-state LSDA.

We thank Ethan Brown for helpful correspondence and for providing the erratum to Ref. [19] prior to publication and Paul Grabowski and Aurora Pribram-Jones for a useful remark. We thank the University of Florida Research Computing Group for computational resources and technical support. V. V. K., J. D., and S. B. T. were supported by U.S. Department of Energy Grant No. DE-SC0002139. T. S. was supported by the Department of Energy Office of Fusion Energy Sciences (FES).

*vkarasev@qtp.ufl.edu

[1] E. W. Brown, B. K. Clark, J. L. DuBois, and D. M. Ceperley, Phys. Rev. Lett. **110**, 146405 (2013).
[2] J. P. Perdew and A. Zunger, Phys. Rev. B **23**, 5048 (1981).
[3] S. H. Vosko, L. Wilk, and M. Nusair, Can. J. Phys. **58**, 1200 (1980).
[4] D. M. Ceperley and B. J. Alder, Phys. Rev. Lett. **45**, 566 (1980).
[5] G. G. Spink, R. J. Needs, and N. D. Drummond, Phys. Rev. B **88**, 085121 (2013).
[6] N. D. Mermin, Phys. Rev. **137**, A1441 (1965).
[7] M. V. Stoitsov and I. Zh. Petkov, Ann. Phys. (N.Y.) **184**, 121 (1988).
[8] R. M. Dreizler in *The Nuclear Equation of State, Part A*, edited by W. Greiner and H. Stöcker (Plenum, New York, 1989), p. 521.
[9] B. Holst, R. Redmer, and M. P. Desjarlais, Phys. Rev. B **77**, 184201 (2008).
[10] F. Lambert, J. Clèrouin, and G. Zèrah, Phys. Rev. E **73**, 016403 (2006).
[11] M. P. Surh, T. W. Barbee III, and L. H. Yang, Phys. Rev. Lett. **86**, 5958 (2001).
[12] V. V. Karasiev, T. Sjostrom, and S. B. Trickey, Phys. Rev. E **86**, 056704 (2012).
[13] V. V. Karasiev, D. Chakraborty, O. A. Shukruto, and S. B. Trickey, Phys. Rev. B **88**, 161108(R) (2013).
[14] S. X. Hu, B. Militzer, V. N. Goncharov, and S. Skupsky, Phys. Rev. B **84**, 224109 (2011).
[15] T. Sjostrom, F. E. Harris, and S. B. Trickey, Phys. Rev. B **85**, 045125 (2012).
[16] R. A. Lippert, N. A. Modine, and A. F. Wright, J. Phys. Condens. Matter **18**, 4295 (2006).
[17] M. Greiner, P. Carrier, and A. Görling, Phys. Rev. B **81**, 155119 (2010).
[18] T. Sjostrom and J. Dufty, Phys. Rev. B **88**, 115123 (2013).
[19] E. W. Brown, J. L. DuBois, M. Holzmann, and D. M. Ceperley, Phys. Rev. B **88**, 081102(R) (2013); **88**, 199901(E) (2013).
[20] R. P. Feynman, N. Metropolis, and E. Teller, Phys. Rev. **75**, 1561 (1949).
[21] V. V. Karasiev, T. Sjostrom, and S. B. Trickey, Phys. Rev. B **86**, 115101 (2012).
[22] S. Tanaka, S. Mitake, and S. Ichimaru, Phys. Rev. A **32**, 1896 (1985).
[23] H. K. Schweng and H. M. Böhm, Phys. Rev. B **48**, 2037 (1993).
[24] F. Perrot and M. W. C. Dharma-wardana, Phys. Rev. B **62**, 16536 (2000); **67**, 079901(E) (2003).
[25] See Supplemental Material at http://link.aps.org/supplemental/10.1103/PhysRevLett.112.076403 for detailed comparisons of the LSDA functional with extended plots and data tables.
[26] S. Tanaka and S. Ichimaru, J. Phys. Soc. Jpn. **55**, 2278 (1986).
[27] S. Tanaka and S. Ichimaru, Phys. Rev. B **39**, 1036 (1989).
[28] S. Ichimaru, Rev. Mod. Phys. **65**, 255 (1993).
[29] F. Perrot and M. W. C. Dharma-wardana, Phys. Rev. A **30**, 2619 (1984).
[30] F. Perrot, Phys. Rev. A **20**, 586 (1979).
[31] H. E. DeWitt, J. Math. Phys. (N.Y.) **7**, 616 (1966).
[32] J. P. Perdew and Y. Wang, Phys. Rev. B **45**, 13244 (1992).
[33] G. L. Oliver and J. P. Perdew, Phys. Rev. A **20**, 397 (1979).
[34] R. M. Dreizler and E. K. U. Gross, *Density Functional Theory* (Springer-Verlag, Berlin, 1990), p. 178.